FACILE FABRICATION OF SILICON NANOPARTICLE LITHIUM-ION BATTERY ANODE REINFORCED WITH COPPER NANOPARTICLES

K. FANG[a,b], M. WANG[a], Y. XIA[a], J. LI[a], Q. JI[a,c], S. YIN[a,d], S. XIE[a], J. BAN[a,b], X. WANG[a], B. QIU[a], Z. LIU[a], C. CHEN[b], Y.J. CHENG[a*]

[a]*Ningbo Institute of Materials Technology and Engineering, Chinese Academy of Sciences, 1219 Zhongguan West Rd, Ningbo, 315201, Zhejiang Province, P. R. China*

[b]*Nano Science and Technology Institute, University of Science and Technology of China, 166 Renai Rd, Suzhou, 215123, Jiangsu Province, P. R. China*

[c]*The University of Nottingham Ningbo China, 199 Taikang East Road, Ningbo, 315100, P. R. China*

[d]*North University of China, Shanglan Rd, Taiyuan, Shanxi Province, 030051, P. R. China*

Studies on the Si based lithium-ion battery anode with long cyclic life and reasonable mass loading density has attracted considerable attention from both academia and industry. A new concept has been developed in this work to enhance the electrochemical performance of the Si nanoparticle anode with high mass loading density (> 1 mg cm^{-2}). Nano-sized Si and Cu particles are dispersed into a Si/Cu nano-composite by facile ultrasonication. For the first time, it is found that the modulus, hardness, and tensile strength of the Si electrode have been significantly improved by the incorporation of the copper nanoparticles, leading to significantly improved cyclic and rate performance. Particularly, the Si/Cu nanocomposite with the Si/Cu mass ratio of 1.0 exhibits a capacity of 1028 $mAhg^{-1}$ after 80 cycles at 0.2 A g^{-1}, which is more than three times higher than that of the bare silicon (328 $mAhg^{-1}$).

(Received November 26, 2016; Accepted April 3, 2017)

Keywords: lithium-ion Battery, Si Nanoparticles, Cu Nanoparticles, Nanoindentation, Mechanical Strength

1. Introduction

Silicon (Si) has been regarded as one of the most promising next generation lithium-ion battery (LIB) anode.[1-6] The high theoretical gravimetric capacity (4200 $mAhg^{-1}$), appropriate working potential (< 0.5 V vs. Li/Li^+), and abundant availability make silicon particularly attractive compared to other LIB anode materials.[7,8] However, the alloying/de-alloying reaction involved with large amount of Li ions causes huge volume expansion (more than 300 %), where serious electrode cracking and pulverization happens. [9-12] Particularly, once the electrode and current collector are disconnected, the reversible capacity will fade rapidly, leading to very poor cyclic performance.[13,14] Developing new concepts to improve the cyclic stability of the Si based LIB anodes has been one of the central issues of the Lithium-ion battery research.

To solve the critical problem of the Si anode, one well-accepted strategy is to exploit nano-sized silicon composited with buffer medium. Among different types of medium, metal is particularly attractive.[15,16] On one hand, the metal possesses excellent mechanical property, which helps to withstand huge volume expansion and absorb mechanical stress. It inhibits the cracking of the individual Si nanoparticles and retards the pulverization process of the whole electrode. On the other hand, the metal also exhibits outstanding electron conductivity. It facilitates the fundamental electrochemical kinetics by providing additional charge carrier transportation path. Nowadays, the

*Corresponding author: chengyj@nimte.ac.cn

frequently exploited synthetic methods for the Si/metal composites are mainly mechanical alloying[17], electrochemical etch[18], magnetron sputtering[19], ion assisted deposition[20,21], electrodeposition[22], These methods are either cost consuming or require delicate control over experimental conditions. Besides, for practical applications, the mass loading density of the Si electrode needs to reach the level of around 1 mg cm^{-2}. It is several times higher than many of the reported values.[23-25] Due to the above reasons it is essential to develop simple and inexpensive fabrication methods to synthesizing Si/metal nanocomposites which improves the cyclic stability of the Si electrode with reasonable mass loading density.

Here in this work, a new concept is proposed to improve the performance of the Si nanoparticle electrode, where copper nanoparticles are used as a reinforcing agent to enhance the mechanical properties of the electrode. Si/Cu nanocomposites are fabricated by directly mixing the silicon and copper nanoparticles through ultrasonication in ethanol, followed by drying process in Fig. 1. The Si/Cu mass ratios are tuned to investigate the impact of the copper nanoparticles on the mechanical properties and electrochemical performance of the electrodes. Particularly, it is worth pointing out that the mass loading density of the Si/Cu nanocomposites are controlled to be more than 1.2 mg cm^{-2}, which provides practical application relevant electrochemical performance of the Si-based lithium-ion battery anode.

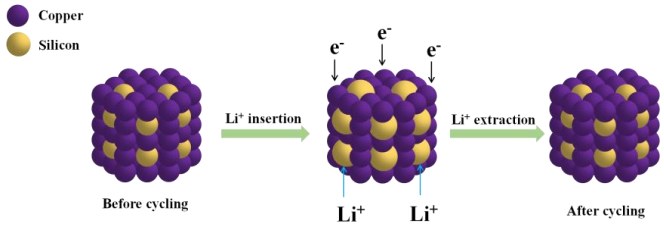

Fig. 1. Schematics of fabrication of the Si/Cu nanocomposite.

2. Experimental Section

2.1. Materials

All of the chemicals were used as received without further purification. Si nanoparticles (30 nm, 99.9 %) were purchased from Haotian Nano Technology (Shanghai) Co., Ltd. Copper nanoparticles (20 nm, 99.9 %) were received from Nanjing XFNANO Material Tech Co., Ltd. Absolute ethanol was obtained from Sinopharm. Corp. Sodium alginate was bought from Aladdin Reagent Co., Ltd., China. Conductive Super P was purchased from SCM Chem. Shanghai, China.

2.2. Sample Preparation and Characterization

Two grams of powder mixtures of pure Cu and Si nanoparticles with different mass ratios of 2.0, 1.0, and 0.5 were dispersed in 30 ml of absolute alcohol. Ultrasonication for 1 hour was applied to homogenize the nanoparticle dispersion, followed by centrifugation at 8000 rpm for 20 min. The samples were collected and dried at 40 °C for 8 hours. And the mass loading density of the electrode is controlled to be more than 1.2 mg cm^{-2}.

The crystallinity of the Si/Cu nanocomposites was investigated by x-ray diffraction (XRD) (Bruker AXS D8 Advance, λ = 1.541 Å, 2.2 kW) with a 2θ ranging from 5 ° to 80 °.

The structures of the electrodes before and after cycling were investigated by field emission scanning electron microscopy (FESEM) with Hitachi S4800 at 4 kV. The samples were mounted to the sample holder with conductive tape and sputtered with gold before imaging. Energy dispersive x-ray spectroscopy (EDX) elemental mapping was performed with FEI QUANTA 250 FEG (America FEI) at an accelerating voltage of 15 kV.

The mechanical properties of the electrodes before cycling were investigated with a MTS G200 nanoindentation system. The Oliver-Pharr method was employed with a continuous stiffness measurement option (Berkovich tip). Four indentation experiments were performed on different spots for each individual sample.

2.3. Electrochemical Measurement

The working electrodes were prepared by manually mixing the Si/Cu nanocomposite, sodium alginate, and super P with the mass ratio of 8:1:1. Water was used as a solvent to form homogeneous slurry, which was spread onto a copper-foil by doctor blading, followed by drying at 80 $^{\circ}$C for 4 h in an air-circulating oven. The dried electrodes were then pressed, and cut into spherical disks with the diameter of 13 mm. The mass loading on the electrode was measured using a balance with the resolution limit of 0.01 mg. After weighing the electrodes were stored in oven at 80 °C before coin cell assembly.

CR 2032 type coin cells were assembled in a glove box (MB-10-compact, MBRAUN) filled with dry argon. Lithium foil was applied as counter electrode and 1 M $LiPF_6$ in a mixed solvent of ethylene carbonate and diethylene carbonate (1:1, v/v) was used as the electrolyte. The rate performance and cyclic performance of the coin cells were tested using a multichannel Land Battery Test System. The rate performance was measured at the current density sequence of 0.1 C, 0.2 C, 0.5 C, 1.0 C and 0.1 C in the voltage range between 3.0 V and 0.005 V (vs. Li/Li^+) (five cycles each current density, 1 C = 1000 $mAhg^{-1}$). The cyclic measurement was carried out at a current density of 0.2 C in the voltage range of 3.0 V − 0.005 V (vs Li/Li^+) for 80 cycles. The specific capacity was calculated on the basis of the total mass of the Si/Cu nanocomposites. The discharge process was defined as the lithiation process, while the charge process was referred to the delithiation process. The CHI 1040B potentiostat/galvanostat analyzer (Shanghai Chenhua instrument Co., Ltd.) was used to carry out the cyclic voltammetry test at a scanning rate of 0.2 mV/s with the voltage range between 0.005 V and 3 V. The electrochemical impedance spectroscopy (EIS) measurements were performed with a frequency range from 100 kHz to 0.01 Hz.

3. Results and discussion

The XRD pattern of the Si/Cu nanocomposite with a representative Si/Cu mass ratio of 1.0 is shown in Fig. 2. The two-theta diffraction peaks at 28.4 °, 47.3 °, 56.1 °, 69.1 ° and 76.4 ° are attributed to the [111], [220], [311], [400] and [331] crystalline planes of the cubic phase of Si (JCPDS No. 77-2111). And the diffraction peaks at 43.5 °, 50.6 °, and 74.3 ° can be indexed as the [111], [200], and [220] crystalline planes of the cubic phase of copper (JCPDS No. 01-1242). Besides the diffraction peaks belonging to the elemental silicon and copper nanoparticles, additional diffraction peaks at 36.6 °, 42.5 °, and 61.7 ° are also observed, which are ascribed to the [111], [200], and [220] crystalline planes of the cubic phase of Cu_2O (JCPDS No.65-3288) due to surface oxidation of the copper nanoparticles.[26]

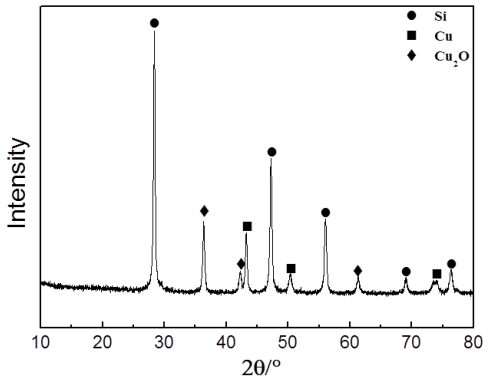

Fig. 2. XRD pattern of the representative Si/Cu nanocomposite with the Si/Cu mass ratio of 1.0.

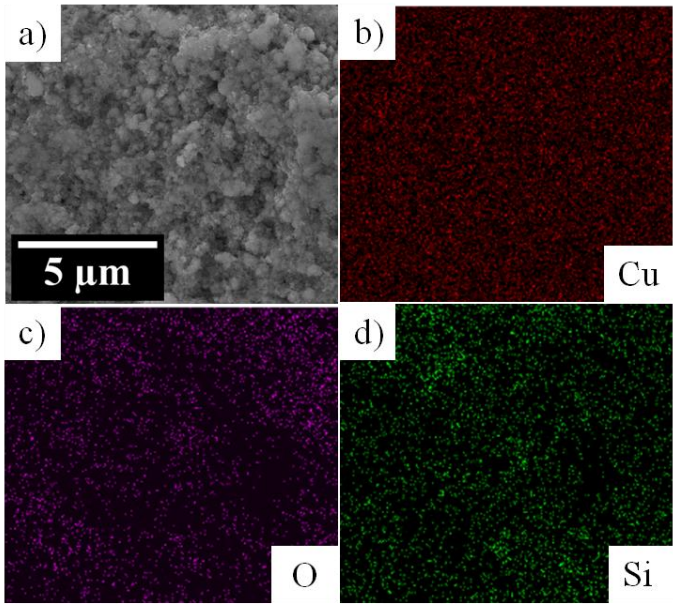

Fig. 3. SEM images of the Si/Cu nanocomposites with the Si/Cu mass ratio of 1.0 (a), and corresponding EDX mapping pictures of the Cu (b), O (c), and Si (d) elements

The morphology and elemental distribution of the Si/Cu nanocomposites with the typical Si/Cu mass ratio of 1.0 are investigated with SEM and EDX as shown in Fig. 3. According to the SEM image of Fig3a, both silicon and copper nanoparticles are homogeneously mixed together, which is further confirmed by the EDX mapping. Based on the EDX results, it is clear that the three element species of silicon, copper, and oxygen are uniformly distributed within the Si/Cu nanocomposite.

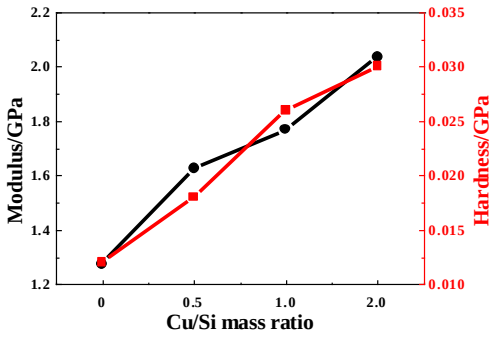

Fig. 4. Modulus and hardness properties of the bare Si and Si/Cu nanocomposite electrodes

The modulus and hardness of the pristine bare Si and Si/Cu nanocomposite electrodes measured by nano indentation are shown in Fig. 4. In general, it is found that the incorporation of the copper nanoparticles significantly enhances the mechanical properties of the electrodes. In details, the modulus and hardness of the Si/Cu nanocomposite electrodes are gradually increased with increasing copper content. Compared to the bare Si electrode, the modulus of the Si/Cu nanocomposite with the Cu/Si mass ratio of 2.0 is significantly increased from 1.276 GPa to 2.036 GPa (by 60 %). Correspondingly, the hardness of the Si/Cu electrode is also effectively lifted from 0.012 GPa to 0.030 GPa with the Cu/Si mass ratio of 2.0, which is 2.5 times higher than that of the bare Si electrode. According to empirical formulae, the tensile strength is approximately equal to one-third of the hardness. It can be assumed that the tensile strength of the Si/Cu nanocomposite electrodes also increases along with increasing copper content. The copper nanoparticles act as a

reinforcing agent to improve the modulus, strength, and hardness of the polymer-bound Si/Cu electrodes.

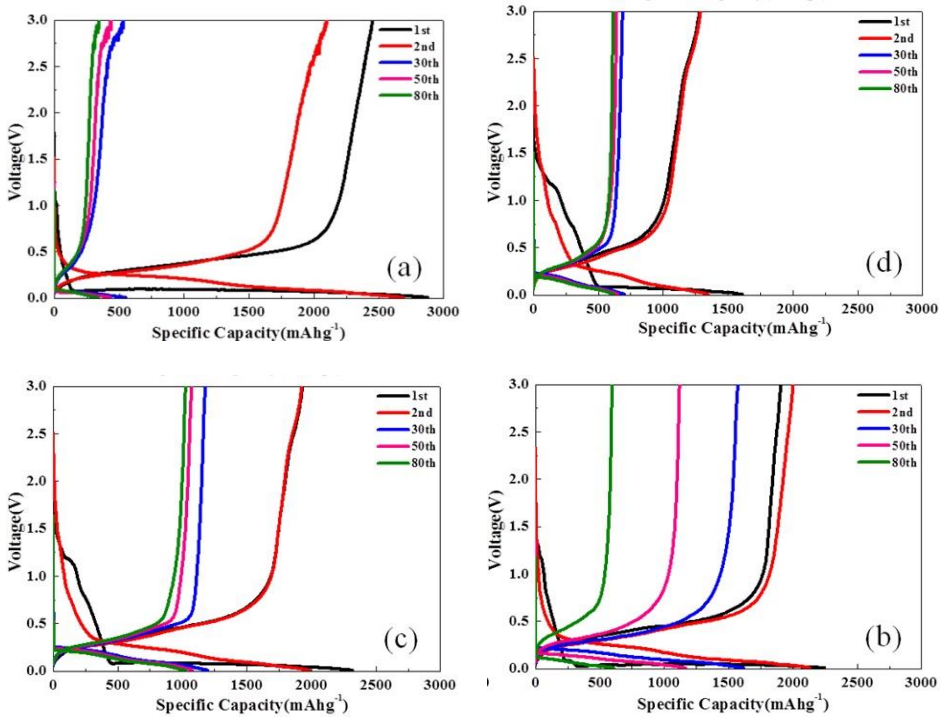

Fig. 5. Discharge/charge curves of the bare Si (a) and Si/Cu nanocomposites with the Si/Cu mass ratio of 2.0, 1.0, and 0.5 (b-d) at the current density of 200 mAg^{-1}.

The discharge/charge curves of the Si/Cu nanocomposites with different Si/Cu mass ratios are shown in Fig. 5. Because the elemental copper is non-active for lithiation and the Cu_2O only possesses moderate capacity, the initial discharge/charge capacities of the Si/Cu nanocomposites are decreased gradually with increasing copper content. Specifically, the initial discharge and charge capacities of the bare Si nanoparticles are 2881 $mAhg^{-1}$ and 2454 $mAhg^{-1}$ respectively, with an initial coulombic efficiency of 85 %. A long flat plateau exists in the first charge process due to the reaction between crystalline Si and Li to form Li_xSi (Fig. 5a). When the Si/Cu mass ratio is decreased to 2.0, 1.0, and 0.5, the discharge/charge capacities are 2242/1907 $mAhg^{-1}$, 2317/1933 $mAhg^{-1}$ and 1610/1280 $mAhg^{-1}$ respectively, corresponding to the initial coulombic efficiency of 85 %, 83 %, and 80 %. The slightly decreased initial coulombic efficiency with high copper content is probably due to the involvement of Cu_2O in the lithiation process. It is well recognized that the transition metal oxide anode is featured with moderate initial coulombic efficiency because of the partial irreversible nature of the lithiation process regarding the conversion reaction mechanism. However, the initial coulombic efficiencies are still kept above 80 % with the addition of the copper nanoparticles. Compared to the bare silicon, the voltage profiles of the Si/Cu nanocomposites exhibit a small plateau at about 1.25 V in the first discharge step, which originates from the lithiation of Cu_2O. [23] However, the plateaus are only observed in the first and second cycle. It implies that the small amount of Cu_2O within the Si/Cu nanocomposites is fully consumed after the first few cycles because the reverse conversion from the elemental copper to Cu_2O is only partial for the delithiation reaction. At the 30^{th} cycle, the capacities of pure Si and Si/Cu nanocomposites with the Si/Cu mass ratio of 2.0 , 1.0 , and 0.5 are 551 $mAhg^{-1}$, 1620 $mAhg^{-1}$, 1199 $mAhg^{-1}$ and 701 mAh^{-1} respectively. It can be seen that the capacity of the pure Si drops much faster than the Si/Cu nanocomposites. After the 30^{th} cycle, the capacity of the pure Si decreases slowly because the absolute value of the capacity is already very limited. On the contrary, the Si/Cu nanocomposite with the Si/Cu mass ratio of 2.0 exhibits a more rapid capacity

fading compared to the Si/Cu mass ratios of 1.0 and 0.5. It means that increasing the copper content can effectively improve the long term cyclic stability of the Si electrode.

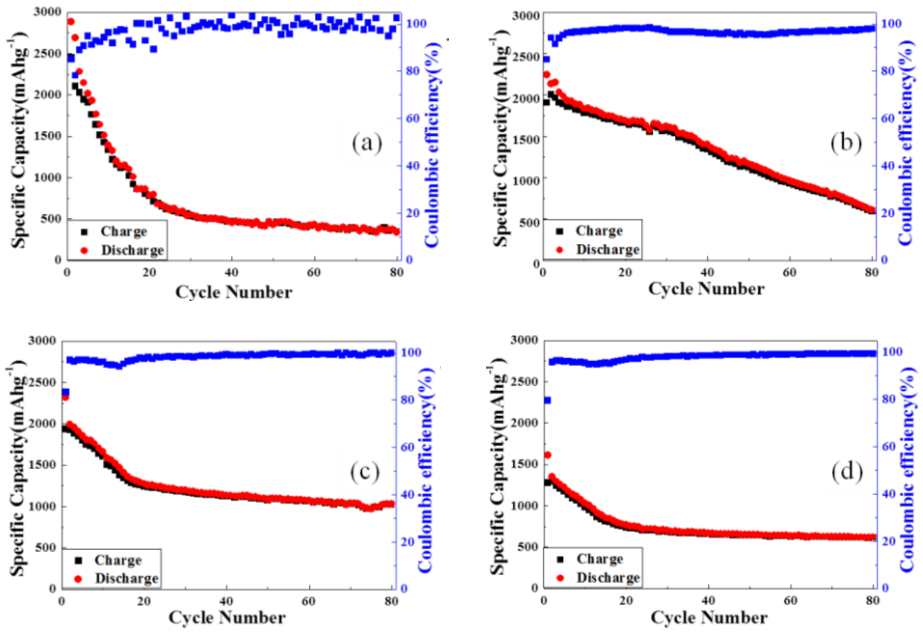

Fig. 6. Cyclic performance of the pure Si (a) and Si/Cu nanocomposites with the Si/Cu mass ratio of 2.0 (b), 1.0 (c), and 0.5 (d)

The cyclic performance of the Si/Cu nanocomposites with different copper contents is given in Fig. 6. In general, the increase of the Cu content improves the cycling stability at the expense of the reversible capacity. The pure Si nanoparticles only retain a capacity of 328 $mAhg^{-1}$ at a current density of 200 mAg^{-1} after 80 cycles despite the high initial discharge capacity of 2881 $mAhg^{-1}$. The rapid capacity decay is mostly related to the drastic volume change of the silicon nanoparticles during repeated lithiation and delithiation processes. When the Si/Cu mass ratio is 2.0, the cycling performance is improved compared with the pure Si nanoparticles. In details, the capacity is over 1600 $mAhg^{-1}$ after the first 30 cycles and it reaches 600 $mAhg^{-1}$ after 80 cycles (Fig. 6b). With the Si/Cu mass ratio further increased to 1.0, even though the initial capacities are slightly decreased, the capacities after 80 cycles are retained at 1028 $mAhg^{-1}$ (Figure 6c). It is a significant improvement compared to the bare silicon anode. Particularly, it is worth emphasizing that the actual mass loading density of the Si/Cu electrode is 1.39 $mgcm^{-2}$, which corresponds to an area capacity density of 1.43 $mAhcm^{-2}$. It is essential to reach the area capacity density of more than 1 $mAhcm^{-2}$, which is one of the key factors for developing practically relevant LIB electrodes. Furthermore, with the Si/Cu mass ratio of 0.5, stable cyclic performance is also observed, which is similar to the Si/Cu nanocomposite with the Si/Cu mass ratio of 1.0 (Figure 6d) . However, the final capacity drops to 621 $mAhg^{-1}$ after 80 cycles because the existence of too much copper nanoparticles. The capacity retention of the bare silicon and Si/Cu nanocomposite electrodes are 11.4 %, 27.2 %, 44.4 %, and 38.6 % with increasing copper content. The gradually increased capacity retention further proves that the cyclic stability of the Si electrode is enhanced by the copper nanoparticles. The improved cyclic performance of the Si/Cu nanocomposites is attributed to the multiple impacts introduced by the copper nanoparticles. Firstly, the addition of the copper nanoparticles significantly improves the modulus, strength, and hardness of the electrodes due to the reinforcing effect. The improved mechanical properties help to maintain the structure integrity of the electrodes, leading to enhanced cyclic performance. Secondly, the copper nanoparticles act as buffer medium to absorb mechanical stress caused by the volumetric change of the silicon nanoparticles because copper possess excellent mechanical strength and ductile ability. The effective stress relief inhibits the fracture and pulverization process of the silicon nanoparticulate

electrode. Thirdly, the copper nanoparticles help to build electronic transportation path along with increasing cycles due to their outstanding electron conductivity. It helps to partially retain capacity even when serious electrode fracture and pulverization take place.

The structure change of the Si/Cu electrodes before and after cycling is investigated by SEM as shown in Fig. 7. Fig. 7a-7d shows the morphology of the Si/Cu electrodes before cycling. Very similar morphologies are observed with different Si/Cu mass ratios, where both silicon and copper nanoparticles are homogeneously mixed together. However, significant morphology change is observed after 80 cycles (Figure 7e-7h). Severe particle agglomeration is observed in the cycled electrodes. Particularly, the bare silicon electrode exhibits more serious agglomeration than the Si/Cu nanocomposite electrodes. The existence of the copper nanoparticle hinders the structure change of the silicon nanoparticles, which helps to retain the reversible capacity.

The rate performance of the Si/Cu nanocomposites with different Si/Cu mass ratios is investigated (Fig. 8). Compared with the bare Si nanoparticles (Figure 8a), the cyclic stability of the Si/Cu nanocomposites under different current densities is significantly enhanced. A considerable improvement of the rate performance under high current density is achieved. Apart from the cycling test at the initial low current density of 100 mAg^{-1} (0.1 C), the specific capacities of all of the Si/Cu nanocomposites are higher than that of the bare silicon. In details, the specific capacity of the pure Si is almost zero under the current density of 0.5 C and 1 C. But the Si/Cu nanocomposites still exhibit the capacities of around 1300 $mAhg^{-1}$ and 400 $mAhg^{-1}$ at 0.5 C and 1 C respectively. Particularly, at the current density of 1000 mAg^{-1}, the specific capacities of the Si/Cu nanocomposites are retained at 447 $mAhg^{-1}$, 824 $mAhg^{-1}$, and 712 $mAhg^{-1}$ respectively with the Si/Cu mass ratio of 2.0, 1.0, and 0.5 (Figure 8b, 8c, and 8d). It is worth pointing out that the mass loading densities of the electrode are controlled to be more than 1.2 $mgcm^{-2}$ for the rate performance test, which are quite high compared to many reported values[23-25]. As the current density is returned back to 100 mAg^{-1}, the specific capacities of the Si/Cu nanocomposites are still better than that of the bare Si electrode. Considering that the bare copper nanoparticles do not contribute to the capacity, it is impressive that the incorporation of the copper nanoparticles significantly improves the rate performance compared to the bare silicon electrode. Even though the addition of copper nanoparticles sacrifices the overall capacity, the copper nanoparticles are supposed to improve the electrical conductivity of the electrode significantly, leading to greatly enhanced rate performance. In particular, the Si/Cu nanocomposite electrode with the Si/Cu mass ratio of 1.0 is found to meet a good balance between sacrificing the overall capacity and improving electron conductivity. Among all the samples, it exhibits average capacities of 2162 $mAhg^{-1}$, 1705 $mAhg^{-1}$, 1258 $mAhg^{-1}$, and 824 $mAhg^{-1}$ at the current densities of 100 mAg^{-1}, 200 mAg^{-1}, 500 mAg^{-1}, and 1000 mAg^{-1} respectively (Fig. 8c).

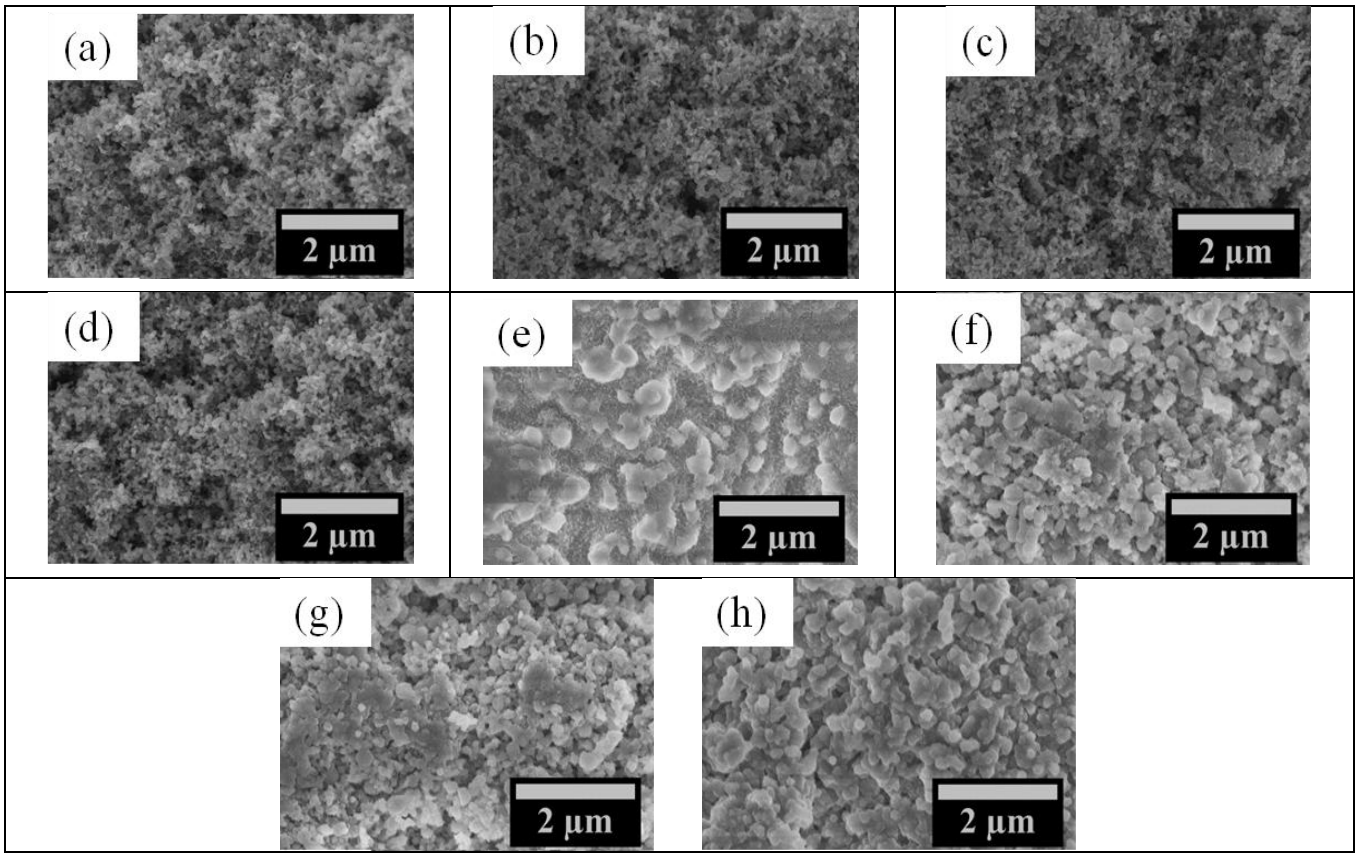

Fig. 7. SEM images of pure Si (a, e) and Si/Cu nanocomposites with the Si/Cu mass ratio of 2.0 (b, f), 1.0 (c, g), and 0.5 (d, h) before and after 80 cycles

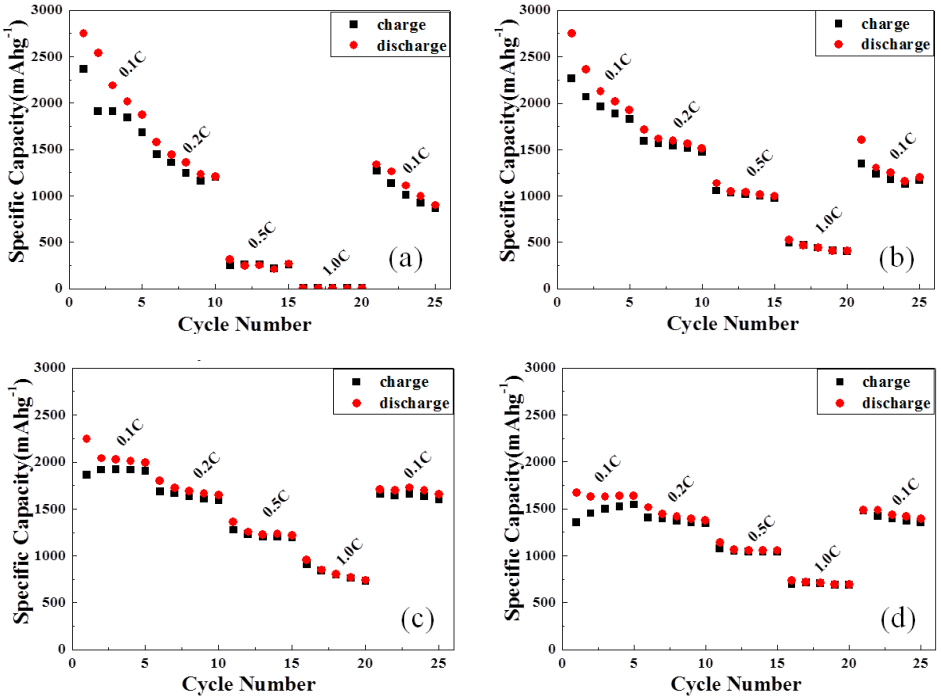

Fig. 8. Rate performance of the bare Si (a) and Si/Cu nanocomposites with the Si/Cu mass ratio of 2.0 (b), 1.0 (c), and 0.5 (d). The current densities are systematically set at 0.1 C, 0.2 C, 0.5 C, 1.0 C and 0.1 C (1 C = 1000 mAg^{-1}). Five cycles are performed for each current density.

Table 1. Comparison of the Si/Cu nanocomposite with the similar work

Current density	Initial coulombic efficiency	Cycle number	Discharge capacity ($mAhg^{-1}$)	Capacity retention	literature	Morphology	
						Si	Cu
0.2 A/g	83 %	80	1028	44 %	this work	particle	particle
0.2 A/g	30 %	100	500	29 %	19	nanocolum	particle
0.4 A/g	54 %	100	815	24 %	20	helices	helices
2.0 A/g	98 %	80	2010	75 %	21	particle	nanorod
0.2 A/g	57 %	60	1646	43 %	22	particle	nanowire
1/12 A/g	76 %	30	850	47 %	27	film	film
0.1 A/g	51 %	100	1628	29 %	28	porous	film
0.1 A/g	98 %.	100	1885	77 %	29	helices	helices

Compared to the electrochemical performance of the representative reported Si/Cu lithium-ion anodes summarized in Table 1, a few conclusions can be drawn. Firstly, the Si/Cu nanocomposite electrodes with the Si/Cu mass ratio of 1:1 possess significantly improved capacity retention than many reported studies.[19,20,27] It indicates that the Si/Cu nanocomposite electrodes synthesized in this work exhibit enhanced cyclic stability. Secondly, morphology of the silicon and copper had certain influence on the battery performance. Thirdly, the mass loading densities of the Si based anodes in these reported work are not seen addressed. However, in our work, the mass loading densities of the Si/Cu electrodes are controlled to be reasonably high, which generates decent total capacity with respect to the individual electrode.

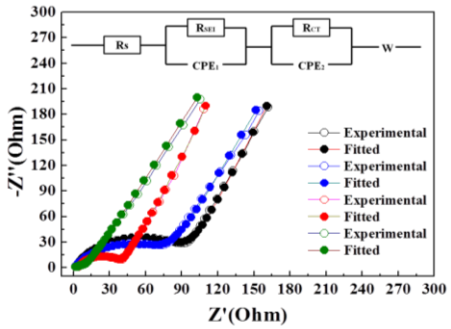

Fig. 9. Experimental and fitting Nyquist plots of the pure Si (black) and the Si/Cu nanocomposites with the Si/Cu mass ratio of 2.0 (olive), 1.0 (red), and 0.5 (blue).

Table 2. Summary of the fitting results of the Si/Cu nanocomposite anodes

Parameter	Pure Si	Si/Cu=2.0	Si/Cu=1.0	Si/Cu=0.5
Rct(Ω)	121.12	77.15	38.74	14.23

Electrochemical impedance spectroscopy (EIS) measurements are carried out to better understand the lithiation/delithiation kinetics of the bare and Si/Cu nanocomposite electrodes. Fig. 9 shows the experimental and fitted Nyquist plots of the bare Si and Si/Cu nanocomposites based on the equivalent Randles model circuit, where the key fitting results are summarized in Table 2. The plots exhibit similar curves consisting of a depressed semicircle in the high-medium frequency and a following line in the low frequency range. The charge transfer resistance (R_{CT}) values of the pure Si and Si/Cu nanocomposites with the Si/Cu mass ratio of 2.0, 1.0, and 0.5 are fitted to be 121.12 Ω, 77.15 Ω, 38.74 Ω and 14.23 Ω respectively (Table 2). The results indicate that the charge transfer resistance decreases along with increasing copper content. A significantly

enhanced charge carrier transportation at the electrode/electrolyte interface is achieved due to the presence of the copper nanoparticles, leading to improved rate performance.[30.31]

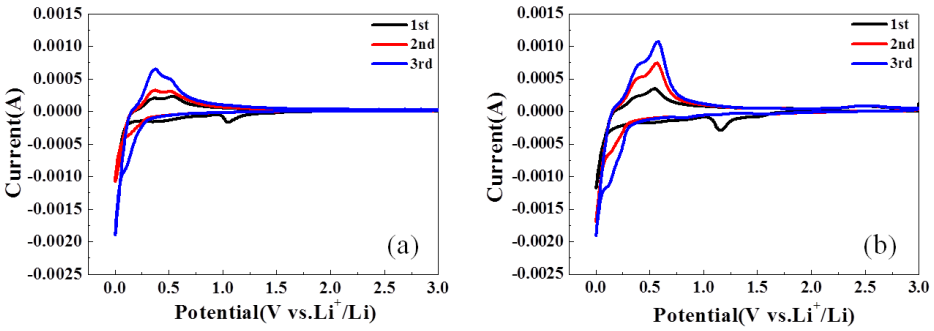

Fig. 10. Cyclic voltammetry profiles of the pure Si (a), and representative Si/Cu nanocomposite with the Si/Cu mass ratio of 1.0 (b) between 0.001 V and 3 V at a scanning rate of 0.2 mV/s.

Cyclic voltammetry (CV) measurement is carried out to investigate the fundamental electrochemical reaction process of the bare silicon and Si/Cu nanocomposite electrodes (Figure 10). In the first cathodic cycle, both pure Si (Figure 10a) and Si/Cu nanocomposites with the Si/Cu mass ratio of 1.0 (Figure 10b) exhibit a strong peak below 0.1 V, suggesting the alloying reaction between Si and Lithium ion.[32] The cathodic peak near 1.1 V is ascribed to the formation of solid electrolyte interface (SEI) layer. In the first anodic process, two peaks at 0.35 V and 0.53 V are observed, which correspond to the extraction of the Lithium ion from the Li-Si alloy. [2,3] Besides, a broad oxidation peak at 2.44 V is found which is associated with the lithiation reaction of Cu_2O in Figure 10b.[33] However, the peak corresponding to the reversed reaction of Cu_2O is not clearly observed. It indicates that the lithiation/delithiation process of Cu_2O is quite limited. It is noteworthy that the characteristic peaks of the pure Si nanoparticles and Si/Cu nanocomposites are located in almost identical positions. The results suggest that the addition of copper nanoparticles does not modify the fundamental electrochemical mechanism of the silicon nanoparticles.

4. Conclusions

A facile method has been developed to synthesize Si based lithium-ion battery anode composited with copper nanoparticles. To our best knowledge, it is for the time to reveal the reinforcing effect of the copper nanoparticles on the mechanical properties of the Si based electrode. It is found that the incorporation of the copper nanoparticles significantly improves the modulus, tensile strength, and hardness of the electrode .With increasing content of the copper nanoparticles, specific capacities increase, followed by decreasing due to decent amount of non-active copper nanoparticles in the electrode. In particular, the Si/Cu nanocomposite electrode with the Si/Cu mass ratio of 1.0 exhibits the highest capacities and good rate performance. The work presented in this manuscript provides a new concept and insight on how to resolve the critical issue of the poor cyclic stability of the Si based lithium-ion battery anode.

Acknowledgement

This research is funded by the Natural Science Foundation of China (51103172), the Zhejiang Nonprofit Technology Applied Research Program (2013C33190), and the open project of the Beijing National Laboratory for Molecular Science (20140138), the CAS-EU S&T cooperation partner program (174433KYSB20150013) and Ningbo Key Laboratory of Polymer Materials.

References

[1] S. Choi, J. C. Lee, O. Park, M.-J. Chun, N.-S. Choi, S. Park, Journal of Materials Chemistry A **1**(36), 10617 **(**2013).
[2] X. Gao, J. Li, Y. Xie, D. Guan, C. Yuan, ACS Appl. Mater. Interfaces **7**(15), 7855 (2015).
[3] H. Tian, X. Tan, F. Xin, C. Wang, W. Han, Nano Energy **11**, 490 (2015).
[4] D. Lin, Z. Lu, P.-C. Hsu, H. R. Lee, N. Liu, J. Zhao, H. Wang, C. Liu, Y. Cui, Energy Environ. Sci. **8**(8), 2371 (2015).
[5] N. Liu, Z. Lu, J. Zhao, M. T. McDowell, H. W. Lee, W. Zhao, Y., Cui, Nat. Nanotechnol. **9**(3), 187 (2014).
[6] J. Zhao, Z. Lu, H. Wang, W. Liu, H. W. Lee, K. Yan, D. Zhuo, D. Lin, N. Liu, Y., Cui, Journal of the American Chemical Society **137**(26), 8372 (2015).
[7] Y. Wang, T. Wang, P. Da, M. Xu, H. Wu, G. Zheng, Advanced Materials **25**(37), 5177 (2013).
[8] J.-Y. Choi, D. J. Lee, Y. M. Lee, Y.-G. Lee, K. M. Kim, J.-K. Park, K. Y. Cho, Advanced Functional Materials **23**(17), 2108 (2013).
[9] G. X. Wang, J. H. Ahn, J. Yao, S. Bewlay, H. K. Liu, Electrochem. Commun. **6**(7), 689 (2004).
[10] H. Guan, X. Wang, S. Chen, Y. Bando, D. Golberg, Chemical communications **47**(44), 12098 (2011)
[11] L. Shi, W. Wang, A. Wang, K. Yuan, Z. Jin, Y. Yang, J. Mater. Chem. A **3**(35), 18190 (2015).
[12] J. Zhang, L. Zhang, P. Xue, L. Zhang, X. Zhang, W. Hao, J. Tian, M. Shen, H. Zheng, J. Mater. Chem. A **3**(15), 7810 (2015).
[13] W. Ren, Z. Zhang, Y. Wang, Q. Tan, Z. Zhong, F. Su, J. Mater. Chem. A **3**(11), 5859 (2015).
[14] B. Liang, Y. Liu, Y. Xu, Journal of Power Sources **267**, 469 (2014).
[15] M. Gauthier, D. Mazouzi, D. Reyter, B. Lestriez, P. Moreau, D. Guyomard, L. Roué, Energy & Environmental Science **6**(7), 2145 (2013).
[16] T. Wada, T. Ichitsubo, K. Yubuta, H. Segawa, H. Yoshida, H. Kato, Nano letters **14**(8), 4505 (2014).
[17] Z. Wen, X. Yang, S. Huang, Journal of Power Sources **174**(2), 1041 (2007).
[18] Z. Yang, D. Wang, F. Li, H. Yue, D. Liu, X. Li, L. Qiao, D. He, Materials Letters **117**, 58 (2014).
[19] B. D. Polat, O. Keles, Electrochimica Acta **170**, 63 (2015).
[20] D. B. Polat, O. Keles, K., Amine, Journal of Power Sources **304**, 273 (2016).
[21] B. D. Polat, O. Keles, Journal of Alloys and Compounds **677**, 228 (2016),
[22] J. Suk, D. Y. Kim, D. W. Kim, Y. Kang, Journal of Materials Chemistry A **2**(8), 2478 (2014).
[23] C. Q. Zhang, J. P. Tu, X. H. Huang, Y. F. Yuan, X. T. Chen, F. Mao, Journal of Alloys and Compounds, **441**(1-2), 52 (2007).
[24] J. Y. Xiang, X. L. Wang, X. H. Xia, L. Zhang, Y. Zhou, S. J. Shi, J. P. Tu, Electrochimica Acta **55**(17), 4921 (2010).
[25] H. Zhang, H. Dong, X. Zhang, Y. Xu, J. Fransaer, Electrochimica Acta **202**, 24 (2016).
[26] S. Uk Son, I. Kyu Park, J. Park, T. Hyeon, Synthesis of Cu2O coated Cu nanoparticles and their successful applications to Ullmann-type amination coupling reactions of aryl chloridesElectronic supplementary information (ESI) available: detailed experimental procedure for the catalytic reactions.. Chemical communications (7), 778 (2004).
[27] B. D. Polat, O. Keles, Thin Solid Films **589**, 543 (2015).
[28] J. Zhang, C. Zhang, S. Wu, Z. Liu, J. Zheng, Y. Zuo, C. Xue, C. Li, B. Cheng, Nanoscale Res. Lett. **11**(1), 214 (2016).
[29] R. Lin, S. Zhang, Z. Du, H. Fang, Y. Ren, X. Wu, RSC Adv. **5**(106), 87090 (2015).
[30] W. Wang, S. Guo, I. Lee, K. Ahmed, J. Zhong, Z. Favors, F. Zaera, M. Ozkan, C. S. Ozkan, Scientific Reports **4**, 4452 (2014).
[31] Y. Zhu, Y. Xu, Y. Liu, C. Luo, C. Wang,. Nanoscale **5**(2), 780 (2013).
[32] N. Lin, J. Zhou, J. Zhou, Y. Han, Y. Zhu, Y. Qian, J. Mater. Chem. A **3**(34), 17544 (2015)
[33] G.-C. Yan, X.-H. Li, Z.-X. Wang, H.-J. Guo, Q. Zhang, W.-J. Peng, Trans. Nonferrous Met. Soc. China, **23**(12), 3691 (2013).